Int. J. Heat Mass Transfer. Vol. 34, No. 7, pp. 1839–1846, 1991
Printed in Great Britain

0017 9310/91 $3.00 + 0.00

The effect of internal heat transfer in cavities on the overall thermal conductivity

DA YU TZOU
Department of Mechanical Engineering, The University of New Mexico, Albuquerque, NM 87131, U.S.A.

(*Received* 16 *March* 1990 *and in final form* 17 *September* 1990)

Abstract—Based on an analytical model, degradation of the overall thermal conductivity is studied in this paper to account for the internal mechanism of heat transfer between the solid medium and the fluid inside cavities. The cavity is assumed to randomly distribute in the solid with its density measured by the volume fraction. The model is capable of characterizing the effect of internal heat transfer such as conductive and convective heat transfer across the surfaces of cavities. In the case involving the convection mode, the Biot number has been identified to be the modulus dominating the overall thermal conductivity, while in the case involving the conduction mode, the ratio of the thermal conductivity of the solid medium to that of the fluid inside cavities is the major influencing factor. The effect of interfacial conduction and convection is found to be pronounced when the volume fraction of pores in the solid exceeds 15%. The large deviation from the experimental result by considering insulated cavities is redeemed by considering heat balance of heat conduction or convection across the cavity surface.

INTRODUCTION

THE OVERALL thermal conductivity of a solid medium containing internal structures such as pores is a complicated subject which depends, in general, on the combined modes of heat transfer between the solid medium and the atmosphere present within the pores. For the porous medium containing thousands of pores with characteristic dimensions ranging from 10 to 100 μm, the *volume fraction* of cavities is the appropriate variable to characterize the overall thermal conductivity rather than the intensified thermal energy cumulated in the neighborhood of individual pores.

A number of theoretical models have been developed to estimate the overall thermal conductivity of porous media. With reference to the thermal conductivity k of the fully dense material, the commonly used models for the estimate of overall thermal conductivity $\bar{k}$ include:

$$\bar{k}/k = 1 - A_1 f, \text{ Loeb [1]} \quad (1)$$

$$\bar{k}/k = (1-f)/(1+f)(A_2 - 1), \text{ Maxwell [2]} \quad (2)$$

$$\bar{k}/k = (1-f)/(1+A_3 f^2), \text{ Koh and Fortini [3]} \quad (3)$$

$$\bar{k}/k = [f^{2/3} + R_R(1-f^{2/3})]/[f^{2/3} - f + R_R(f+1-f^{2/3})], \text{ Russell [4]} \quad (4)$$

$$\bar{k}/k = [1+2f(1-R_R)/(2R_R+1)]/[1-f(1-R_R)/(2R_R+1)], \text{ Eucken [5]} \quad (5)$$

$$\bar{k}/k = 1 - f, \text{ Francl and Kingery [6]} \quad (6)$$

$$\bar{k}/k = \{2 - 3[1-(1-f)^n](1-f)\}/(2+f), \text{ Murabayashi } et\ al. \text{ [7]} \quad (7)$$

with f being the volume fraction of pores and R_R the ratio of thermal resistance of the fluid inside cavities to that of the solid medium. Mathematically, $R_R = R_f/R = k/k_f$. The coefficients of A in equations (1)–(3) were recently determined [8] for the P304L stainless steel atomized metal powder. Under normal conditions, it has been found that the mean deviation of the experimental data for the Loeb and Russell models is less than 10%, while in the case that the cylindrical pore axis (the effect of pore orientation) is perpendicular to the direction of heat flow, the Eucken and Russell models do not yield satisfactory results. Also, the Maxwell, Murabayashi *et al.*, and Loeb models were evaluated by El-Fekey *et al.* [9] on thoria compacts with porosities ranging from 19 to 46% in the temperature range from 500 to 900°C. Comparison with experimental results is necessary for theoretical models due to the complicated nature of heat transfer through the porous media. Experimentally, the comparative method for determining the overall thermal conductivity was widely used by researchers [10–12]. The way to minimize the errors induced by the method has also been discussed extensively [13–15].

The analytical model proposed in ref. [16], based on the self-consistent approach [17–20], is worthy of a mention. The model is developed on a continuum basis which absorbs the effect of cavities on the overall degradation of thermal conductivity in an added thermal resistance tensor. The added tensor thus formulated depends on the temperature distribution along the surface of the cavity which can be calculated analytically for cavities with a simple geometry or numerically for cavities with complicated geometry. Whether the cavity is insulated or subjected to energy

NOMENCLATURE

- a characteristic dimension of the internal cavity [m]
- e unit normal vectors along the coordinate axes
- f volume fraction of the internal cavities
- g temperature function per unit heat flux [m^2 K^{-1} W^{-1}]
- H added tensor in the overall thermal resistance tensor [m K^{-1} W^{-1}]
- k thermal conductivity [W m^{-1} K^{-1}]
- n unit normal vector of the crack surface
- N total number of cracks per unit volume
- r position vector of a material point around the spherical cavity [m], radial distance measured along the crack surface from the center of the crack [m]
- S boundary surface of the entire body [m^2]
- T temperature [K]
- x spatial coordinates [m]
- y coordinate perpendicular to a line crack.

Greek symbols

- β transformation matrix between the prime and the physical coordinate systems
- δ Kronecker delta function
- θ Euler angle [deg]
- Θ orientation angle in the spherical coordinate system [deg]
- ϕ Euler angle [deg]
- Φ orientation angle in the spherical coordinate system [deg].

Subscripts and superscripts

- X_i component of vector X in the x_i-direction, $i = 1, 2, 3$
- X_R ratio of the quantity X of the matrix to that of the fluid inside cavities
- X_{ij} indicial notation for the tensorial quantity X
- $X_{,i}$ $\partial X/\partial x_i$
- X^C physical quantity X in the cavity
- $\bar{X}$ volumetric average of X
- X' prime coordinates aligned to the cavity
- X^{-1} inverse of X.

exchange with the fluid inside the cavity, therefore, has an intrinsic influence on the outcome of the overall thermal conductivity. Also, in the case that the intact behavior of the solid medium is highly directional or the incoming heat flux is multi-dimensional, the model is capable of predicting an *anisotropic* overall thermal conductivity tensor in a natural fashion.

Application of the model to predict the overall degradation of thermal conductivity in a solid medium containing insulated cavities has already been made [16]. In the range with volume fraction greater than 15%, however, the predicted values of overall thermal conductivity start to deviate from the experimental result. As the volume fraction of pores increases to 40%, the analytical result is approximately 30–40% lower than that obtained experimentally. In improving the established model to predict the degradation of overall thermal conductivity for media with higher values of porosity, therefore, the present study aims to redeem such a difference by incorporating the modes of internal heat transfer across cavity surfaces.

THE ANALYTICAL MODEL

The detailed formulation for weakening of a Fourier solid carrying thermal energy due to the presence of internal cavities is provided in the previous work [16]. In summary, the model absorbs the effect of internal cavities in an added tensor H_{ij} as shown by

$$\bar{R}_{ij} = R_{ij} + H_{ij}(\bar{R}_{ij}), \quad \text{for } i, j = 1, 2, 3 \tag{8}$$

where R_{ij} is the thermal resistance tensor of the fully dense material and $\bar{R}_{ij}$ the overall thermal resistance tensor of the porous medium which is the reciprocal of the overall thermal conductivity tensor, $\bar{R}_{ij} = \bar{k}_{ij}^{-1}$. Determination of the $\bar{R}_{ij}$ tensor according to equation (8) obviously depends upon the added tensor H_{ij}. Through the concept of Green's function and the assistance of the divergence theorem, it has been shown analytically that the H_{ij} tensor is governed by

$$\int_{S^C} T n'_i \, \mathrm{d}S^C = H'_{ij} \bar{q}'_j \tag{9}$$

where S^C is the surface area of the cavity, n'_i the unit normal vector of the cavity surface in the x'_i-direction, T the temperature, and $\bar{q}'_j$ the incoming heat flux components along the x'_j-direction. The prime coordinate system is aligned according to the relative direction of the incoming heat flux to the special geometry of cavities under consideration. For a solid containing penny-shaped cracks as illustrated in Fig. 1(a), for example, the temperature distribution T in equation (9) is determined from the prime coordinate system such that the incoming heat flux component $\bar{q}'_3$ is perpendicular to the crack surface. For the present problem illustrated in Fig. 1(b), the incoming heat flux component $\bar{q}'_3$ is taken to be perpendicular to the spherical cavity, which is actually arbitrary due to perfect symmetry of the spherical surface. Based on the tensor transformation for the base vectors $\mathbf{e}'_i$ from

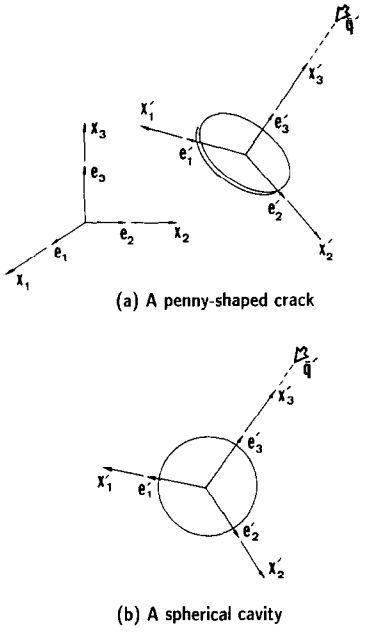

FIG. 1. The prime and global coordinate systems assigned for (a) a penny-shaped crack and (b) a spherical cavity.

the prime coordinate system back to those of the global coordinate system $\mathbf{e}_i$

$$\mathbf{e}_i = \beta_{ij}\mathbf{e}'_j \tag{10}$$

with

$$\beta_{ij} = \begin{bmatrix} -\sin\theta & -\sin\phi\cos\theta & \cos\phi\cos\theta \\ \cos\theta & -\sin\phi\sin\theta & \cos\phi\sin\theta \\ 0 & \cos\phi & \sin\phi \end{bmatrix} \tag{11}$$

and θ and ϕ the Euler angles, then, the added tensor H_{ij} in the global coordinate system is obtained by averaging the H'_{ij} tensor over all the possible orientations of the cavity relative to the incoming heat flux, i.e.

$$H_{ij} = \frac{N}{2\pi}\int_0^{2\pi}\int_0^{\pi/2} \beta_{im}\beta_{jn}H'_{mn}(\bar{R}_{ij})\cos\phi\,\mathrm{d}\phi\,\mathrm{d}\theta,$$

$$\text{for } i,j,m,n = 1,2,3. \tag{12}$$

Clearly, the most important component in this approach is the determination of the temperature field around the cavity. Once the temperature field is determined in terms of the heat flux $\bar{q}'_i$ incoming from the x'_i-direction

$$T(x'_i) = g_i(x'_i)\bar{q}'_i \tag{13}$$

the components of H'_{ij} can be determined from equation (9)

$$H'_{ij} = \int_{S^C} g_j^B n'_i\,\mathrm{d}S^C \tag{14}$$

where g_j^B are the boundary values of the functions g_j at the cavity surface. With the coefficients β_{ij} defined in equation (11) and the H'_{ij} tensor determined from equation (14), the components of H_{ij} can thus be calculated from equation (12). In passing to the examples illustrating this standard procedure, it should be noticed that the added tensor H_{ij} calculated in this manner may not always be a diagonal matrix. The resulting overall thermal resistance tensor, and hence its reciprocal being the overall conductivity tensor, calculated according to equation (8) may present nonzero values in the off-diagonal terms and the overall conductivity tensor may consequently become anisotropic. In the present model, whether the overall conductivity tensor is anisotropic or not depends on the intact behavior of the thermal conductivity, the geometrical configuration of cavities, and the thermal loading imposed on the system.

SPHERICAL CAVITIES

The value of the analytical model proposed in the present work lies in its universality in estimating the overall thermal conductivity. The effect of internal heat transfer across the surface of cavities is reflected by the boundary values of the g_j-functions, g_j^B, in equation (14). It is indeed the boundary temperature at the surface of cavities defined in equation (13). In addition to the g_j-functions, the overall thermal resistance depends also on the shape of the cavity which is reflected by the unit normal vectors n'_i and the differential surface area $\mathrm{d}S^C$ of the specific cavity surface under consideration. In the sequel we shall illustrate the use of equations (8)–(14) by calculating the overall thermal conductivity of a solid containing spherical cavities subjected to various modes of heat transfer across the surface.

The incoming heat flux $\bar{q}'_3$ in a three-dimensional solid is assumed to be disturbed by spherical cavities with an average radius a as shown in Fig. 2. The unit normals at the surface of the spherical cavity are expressed by

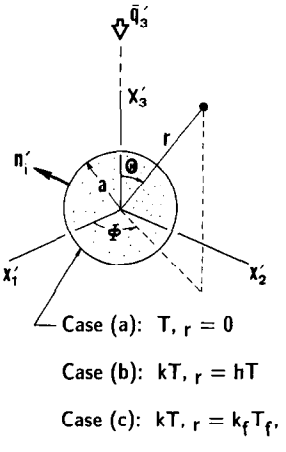

FIG. 2. A spherical cavity subjected to a uni-directional heat flux in the x'_3-direction.

$$n_i' = x_i'/a, \quad \text{with } i = 1, 2, 3 \tag{15}$$

where prime coordinates x_i' are related to the spherical coordinates (r, Θ, Φ) by

$$\{x_1', x_2', x_3'\} = \{r \sin\Theta \cos\Phi, r \sin\Theta \sin\Phi, r \cos\Theta\} \tag{16}$$

and the differential surface dS' is $a^2 \sin\Theta \, d\Theta \, d\Phi$. Also, we assume the heat flux $\bar{q}_3'$ is in the same sense as the unit normal $\mathbf{e}_3'$ but in the opposite direction. The intact thermal resistance tensor of the medium is assumed to be isotropic

$$R_{ij} = R\delta_{ij}, \quad \text{for } i, j = 1, 2, 3 \tag{17}$$

with δ_{ij} being the Kronecker delta function and R the isotropic thermal resistance of the solid, the reciprocal of the isotropic thermal conductivity $1/k$.

For a spherical cavity with Φ-symmetry, the harmonic function resulting from the steady-state energy equation is

$$T = (Ar + B/r^2) \cos\Theta \tag{18}$$

with A and B being coefficients depending on the boundary conditions at the cavity surface. At a distance far away from the cavity, the heat flux resulting from equation (18) must be identical to the incoming heat flux $\bar{q}_3'$, which gives

$$\bar{q}_3' = k(\partial T/\partial x_3) \quad \text{as } r \to \infty. \tag{19}$$

By noticing that $x_3 = r \cos\Theta$ according to the coordinate system defined in Fig. 2, equations (18) and (19) yield

$$A = \bar{q}_3'/k = \bar{q}_3' R. \tag{20}$$

The coefficient B depends on the boundary condition at the surface of the cavity which reflects a specific mode of heat transfer across the interface. In this work, we shall consider three examples: (a) spherical cavities with insulated boundaries, (b) spherical cavities with convective heat transfer across the surface, and (c) spherical cavities with conductive heat transfer across the surface. Case (b) is to illustrate the effect of heat transfer coefficient on the overall thermal conductivity while Case (c) is to study the effect of relative thermal conductivity.

(a) *Insulated spherical cavities.* The insulated boundary condition at the surface of the cavity in this case is expressed by

$$T_{,r} = 0 \quad \text{at } r = a. \tag{21}$$

Substituting equation (20) into equation (18) and the result into equation (21), the coefficient B is determined as

$$B = \bar{q}_3' R a^3/2 \tag{22}$$

and the temperature distribution is determined as

$$T(r, \Theta) = (\bar{q}_3' R)(r + a^3/2r^2) \cos\Theta. \tag{23}$$

Equation (23) is exactly the same as that used by Florence and Goodier [21]. Referring to equation (13), the g_j-functions are thus

$$g_1 = g_2 = 0, \; g_3(r, \Theta, \Phi) = R(r + a^3/2r^2) \cos\Theta,$$
$$\text{and } g_3^B = g_3(a, \Theta, \Phi) = (3aR/2) \cos\Theta. \tag{24}$$

Substituting equations (15), (16), and (24) into equation (14) and integrating the cavity surface for $\Theta \in [0, \pi]$ and $\Phi \in [0, 2\pi]$, the components of H_{ij}' can be integrated immediately to give

$$H_{33}' = 2\pi a^3 \bar{R} \quad \text{and } H_{ij}' \text{ otherwise.} \tag{25}$$

The tensor H_{ij}' thus obtained is then transformed back to the physical coordinates x_i according to equation (12). The result is

$$H_{ij} = \frac{2\pi}{3} \bar{R} f \delta_{ij}, \quad \text{for } i, j = 1, 2, 3 \tag{26}$$

where the total number of cavities in a material volume with the characteristic dimension a, Na^3, corresponds to the volume fraction f of cavities [16, 20] in the solid. The overall thermal resistance $\bar{R}$, finally, is determined by substituting equation (26) into equation (8), which gives

$$R/\bar{R} = \bar{k}/k = 1 - (2\pi/3) f \tag{27}$$

with $\bar{R}$ being the principal components of $\bar{R}_{ij} = \bar{R}\delta_{ij}$ as a result of equation (17). This is the desired equation for the overall thermal conductivity of a solid medium containing insulated spherical cavities. It turns out to be an isotropic tensor under the present condition with randomly oriented spherical cavities and a uni-directional incoming heat flux. The isotropy of the overall thermal conductivity tensor results from zero values of the g_1 and g_2 functions in equation (24), which consequently reduces an H_{ij}' tensor with H_{33}' being the only non-zero component as shown by equation (25). For cavities with an anisometric shape such as a penny-shaped crack subjected to multi-directional heat flux impingement as illustrated in Fig. 1(a), this may not be the case and an anisotropic overall thermal conductivity tensor would result.

(b) *Spherical cavities with interfacial convection.* The second case under consideration involves heat balance between the solid medium and the fluid phase trapped in the cavity across the cavity surface. Mathematically, this condition can be expressed by

$$kT_{,r} = hT \quad \text{at } r = a \tag{28}$$

where h is the averaged heat transfer coefficient and the temperature of the fluid inside the cavity is assumed to be zero without loss in generality. With the result of the coefficient A shown in equation (20), combination of equation (18) with equation (28) yields

$$B = \bar{q}_3' R a^3 (1 - haR)/(2 + haR) \tag{29}$$

and the temperature distribution

$$T(r, \Theta) = (\bar{q}_3' R)[r + a^3(1 - haR)/(2 + haR)r^2] \cos\Theta \tag{30}$$

is obtained. The rest of the procedure is exactly the same as that in the previous case and the corresponding equations are summarized as follows:

The g_j-functions

$$g_1 = g_2 = 0,\ g_3(r,\Theta,\Phi) = R(r+a^3/2r^2)\cos\Theta,$$
$$\text{and } g_3^B = g_3(a,\Theta,\Phi) = [3aR/(2+haR)]\cos\Theta. \tag{31}$$

The H'_{ij} tensor in the prime coordinate system x'_i

$$H'_{33} = 4\pi a^3\bar{R}/(2+h\bar{R}a) \quad \text{and } H'_{ij} \text{ otherwise.} \tag{32}$$

The H_{ij} tensor in the global coordinate system x_i

$$H_{ij} = \frac{4\pi\bar{R}f}{3(2+h\bar{R}a)}\delta_{ij}. \tag{33}$$

Substituting equation (33) into equation (8) then yields the following equation for the determination of the overall thermal resistance $\bar{R}$:

$$(3ha)\bar{R}^2+(6-3haR-4\pi f)\bar{R}-6R = 0. \tag{34}$$

Again, the overall thermal resistance tensor is isotropic in this case. In contrast to equation (27) in Case (a), equation (34) is a quadratic equation to be solved for $\bar{R}$. By introducing the Biot number defined as $Bi = ha/k = haR$, its solution can be arranged in the form of

$$\frac{\bar{k}}{k} = \frac{R}{\bar{R}} = \frac{6Bi}{(3Bi+4\pi f-6)+\sqrt{((Bi+4\pi f-6)^2+72Bi}} \tag{35}$$

where the negative root is dropped because the thermal conductivity is positive definite. In the present case with convection heat transfer across the surface of cavities, equation (35) shows that the overall degradation of the thermal conductivity is characterized by the Biot number. With the numerical values provided in Table 1, Fig. 3 graphically displays the variation of the ratio of $\bar{k}/k$ vs the volume fraction f. When the Biot number is small, say 2×10^{-5}, the fluid inside the cavity only carries a small amount of energy and the cavity behaves like being insulated. The result of $\bar{k}/k$ represented by equation (35) in this case reduces to

Table 1. Numerical values of $\bar{k}/k$ varying as a function of the volume fraction f. Case (b) with heat convection across the cavity surface

Volume fraction f	Overall thermal conductivity $\bar{k}/k$		
	$Bi = 2\times10^{-5}$†	$Bi = 0.2$	$Bi = 2$
0	1	1	1
0.1	0.79	0.81	0.90
0.2	0.58	0.64	0.81
0.3	0.37	0.48	0.73
0.4	0.16	0.39	0.67

† The case corresponding to $\bar{k}/k = 1-(2\pi/3)f$ for insulated cavities.

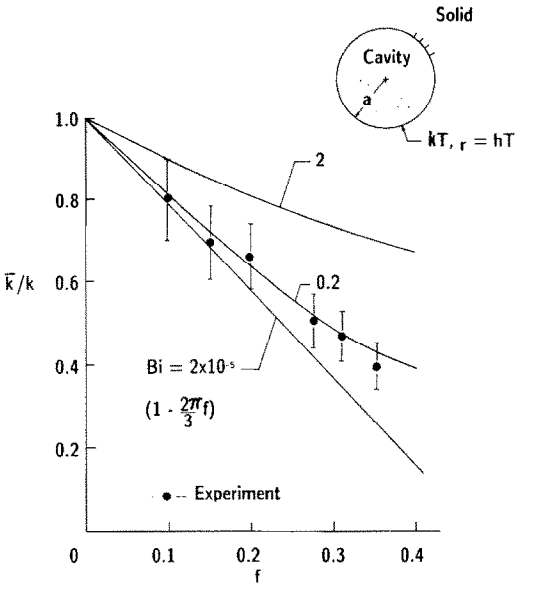

FIG. 3. The effect of Biot number on the degradation of overall thermal conductivity, equation (35). Experimental results are from Agapiou and DeVries [8].

equation (27) for insulated cavities, as represented by the straight line $\bar{k}/k = 1-(2\pi/3)f$. When Biot number increases, as expected, the relative strength of heat convection increases and the overall thermal conductivity increases consequently. The relationship between $\bar{k}/k$ and f becomes more nonlinear especially in the range with larger values of f. By comparing this example with the previous case with insulated cavities, we thus conclude that the heat convection across the cavity surface is a non-linear effect to the overall thermal conductivity. The experimental results recently obtained by Agapiou and DeVries [8] are also displayed for comparison. The reported values of $\bar{k}/k$ in their work are up to 40% of the porosity. The model employing insulated cavities is sufficient within the range of f being approximately 15%. For the solid with larger values of volume fraction than this threshold, the convection mode of heat transfer across the cavity surface becomes important as reflected by the curve with $Bi = 0.2$ in the figure which agrees well with the experimental results in the full range of the volume fraction f. The Biot number, as shown by equation (35), appears as a parameter which has been given arbitrary values in comparison with the experimental results of $\bar{k}/k$ vs f. On a numerical basis, the purpose is to determine the threshold value of Bi such that the predictability of the model could be extended to the range with higher values of porosity. In direct experimental measurements, however, the effects of other modes of internal heat transfer such as heat conduction and radiation across the cavity surfaces may also be included as an entirety. For direct comparisons, therefore, the parameters involved in this model such as the values of h, k, and a (and hence the value of the Biot number) must be determined first

and then substituted into equation (35) for determining the overall thermal conductivity. This is also the situation in the next section where the effect of thermal conductivity of fluids trapped in cavities is studied.

(c) *Spherical cavities subject to conductive heat exchange.* The third case under consideration involves conductive energy balance across the cavity surface. The stationary fluid inside cavities is simulated as a thermal field which exchanges the energy with the solid medium by heat conduction. The energy equations for the solid medium and the fluid phase inside cavities are both Laplacian and the harmonic functions for temperature distributions are

$$T = (\bar{q}'_3 Rr + B/r^2)\cos\Theta, \text{ for the solid medium with } r > a \quad (36)$$

$$T_f = Cr\cos\Theta, \text{ for the fluid phase inside the cavity with } r < a \quad (37)$$

where the boundary condition at infinity, equation (19), has been used in equation (36) and the term containing $1/r^2$ in equation (37) has been dropped because the fluid temperature must keep bounded at $r = 0$. The coefficients B and C in equations (36) and (37) are determined from the continuity of temperature and heat flux across the surface of the cavity

$$T = T_f \quad \text{and} \quad (1/R)T_{,r} = (1/R_f)T_{f,r} \quad \text{at } r = a. \quad (38)$$

From equations (36) and (37), then, equation (38) renders

$$B = \bar{q}'_3 R[a^3(R_f - R)/(R+2R_f)] \quad \text{and}$$
$$C = \bar{q}'_3 R[3R_f/(R+2R_f)] \quad (39)$$

and the temperature field in the solid medium and fluid phase are completely determined. The corresponding equations for calculating the overall thermal conductivity in this case are:

The g_i-functions

$$g_1^R = g_2^R = 0 \quad \text{and} \quad g_3^R = [3aRR_f/(R+2R_f)]\cos\Theta. \quad (40)$$

The H'_{ij} tensor in the prime coordinate system x'_i

$$H'_{33} = 4\pi a^3 \bar{R}R_f/(\bar{R}+2R_f) \quad \text{and} \quad H'_{ij} = 0 \text{ otherwise.} \quad (41)$$

The H_{ij} tensor in the global coordinate system x_i

$$H_{ij} = \frac{4\pi f \bar{R}R_f}{3(\bar{R}+2R_f)}\delta_{ij}. \quad (42)$$

Substituting equation (42) into equation (8) then yields a quadratic equation for determining the overall thermal resistance $\bar{R}$

$$3\bar{R}^2 + (6R_f - 3R - 4\pi f R_f)\bar{R} - 6RR_f = 0 \quad (43)$$

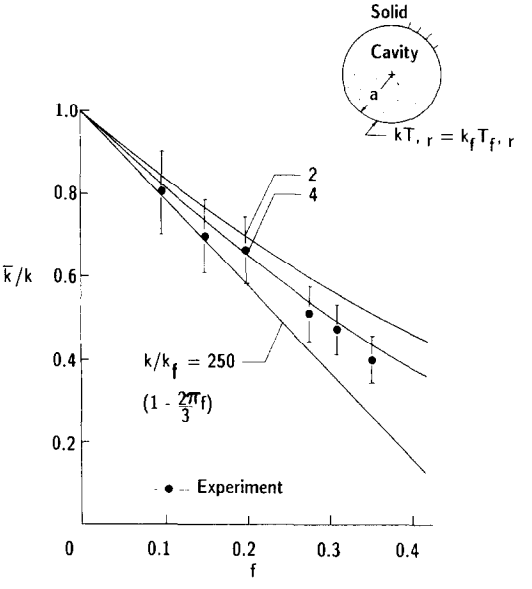

FIG. 4. The effect of relative thermal conductivity k/k_f on the overall thermal conductivity, equation (44). Experimental results are from Agapiou and DeVries [8].

which can be solved for the ratio of the overall thermal conductivity to its intact value

$$\frac{\bar{k}}{k} = \frac{R}{\bar{R}} = \frac{6}{(3+4\pi f R_R - 6R_R)+\sqrt{((3+4\pi f R_R - 6R_R)^2+72R_R)}}$$
$$\text{with } R_R = R_f/R = k/k_f. \quad (44)$$

Note the similarity between equations (35) and (44). The relationship between $\bar{k}/k$ and f is again nonlinear under the conductive mode of heat transfer across the cavity surface, as shown by Fig. 4. When the value of k_f is small relative to the intact value of the solid, say $k/k_f \simeq 250$, the cavity behaves like it is insulated and the result represented by equation (54) reduces to that of equation (27) for insulated cavities. As the value of $R_R(k/k_f)$ decreases, equivalently the value of k_f increases and the overall thermal conductivity of the solid increases. Note also that the curve with $k/k_f = R_R = 4$, as provided in Table 2, gives the values

Table 2. Numerical values of $\bar{k}/k$ varying as a function of the volume fraction f. Case (c) with heat conduction with the fluid inside cavities

Volume fraction f	Overall thermal conductivity $\bar{k}/k$		
	$R_R = 2$	$R_R = 4$†	$R_R = 250$‡
0	1	1	1
0.1	0.84	0.82	0.79
0.2	0.69	0.65	0.58
0.3	0.56	0.50	0.38
0.4	0.46	0.37	0.17

† The case close to Case (b) with $Bi = 0.2$.
‡ The case corresponding to $\bar{k}/k = 1-(2\pi/3)f$ for insulated cavities.

of $\bar{k}/k$ very close to those in the previous Case (b) with $Bi = 0.2$. The models simulating heat conduction and convection across the cavity surface are thus interrelated.

CONCLUSION

The effect of interfacial convection and conduction across the cavity surface on the overall thermal conductivity of porous media has been investigated in this work. The Biot number has been found to be the physical modulus characterizing the effect of heat convection, while the ratio of thermal conductivity of the solid medium to that of the fluid phase inside cavities, k/k_f, has been found to characterize the effect of heat conduction. In both cases, the analytical results obtained in this work agree well with the experimental data for $Bi = 0.2$ in the convection model and $k/k_f = 4$ in the conduction model. In comparison with the results employing insulated cavities [16], consideration of internal heat transfer across cavity surfaces significantly extends the applicable range of the model to solid media with porosity being at least 40%.

The analytical model proposed in this work is general enough to study cavities of any shape. With temperature around a single cavity being the central quantity in this model, however, numerical methods such as the finite difference or the finite element method may be needed for cavities with an irregular geometry. In this case, the surface integral of temperature, and hence the components of the H'_{ij} tensor in equation (9), must be evaluated numerically due to the absence of an analytical form for the temperature distribution T along the cavity surface. At this stage of the development, there exists two major restrictions in the model being proposed. First, the volume fraction or porosity of cavities in the solid cannot be too high because interactions with adjacent cavities are not incorporated in determining the temperature distributions represented by equations (23), (30), and (36). Should the coupling effects among cavities be included, the problem would involve two cavities separated by a distance l in the mathematical formulation and the value of l will be the additional geometrical parameter involved in the temperature distribution along the cavity surface. In averaging the Euler angles ϕ and θ to obtain the H_{ij} tensor according to equation (12), then, the one averaging the distance l over the corresponding physical domain from l_1 (the smallest value of l between any adjacent cavities) to l_2 (the largest value of l between any adjacent cavities) should also be included and the overall thermal conductivity in this case will depend on the values of l_1 and l_2. Because the problem formulated in this manner involves a multiply-connected region, numerical methods seem to be unavoidable in determining the temperature distribution. Secondly, because determination of the components of the H'_{ij} tensor is made by comparing the coefficients of $\bar{q}'_j$ in equation (9), application of the present model is limited to linear problems for which the temperature T can be represented by a *linear* function of the incoming heat flux. For non-linear problems such as the one involving a temperature-dependent thermal conductivity, the temperature distribution T around the cavity depends also on the higher order terms of $\bar{q}'_j$ and at this stage of the development, the model is not mature yet for such extensions.

Whether the overall thermal resistance tensor is kept isotropic or not fully depends on the outcome of the added tensor H_{ij}. In the present case with randomly oriented spherical cavities subjected to a unidirectional heat flux, the H_{ij} tensor, and hence the $\bar{R}_{ij}$ tensor, turns out to be isotropic. In the case that H_{ij} becomes an anisotropic tensor, such as that resulting from the presence of a multi-directional incoming heat flux impinging on cavities with an anisometric shape, a total of nine components may appear altogether in the overall thermal resistance tensor $\bar{R}_{ij}$. Besides, equations (27), (35), and (44) are obtained based upon an isotropic medium. Should an originally anisotropic material be considered, the temperature distribution may involve all the components R_{ij} of the thermal resistance tensor, and equation (8) may lead to a total of nine algebraic equations to be solved for all the components of $\bar{R}_{ij}$.

The overall thermal conductivity is a combined result of thermal loading, geometrical configuration of cavities, and intact behavior of the solid medium. It reflects the thermal response of a porous medium to a specific way with which the medium is excited. The complicated interaction among the three factors of loading, geometry, and material may render an anisotropic tensor for the overall thermal conductivity. The distribution of penny-shaped mesocracks in a preferential direction in a solid medium [16], for example, may render a smaller value of the thermal conductivity in the direction perpendicular to the crack surface in comparison with that in parallel due to the discontinuity across the crack surface. Along with the extensions of the model into the non-linear problems with or without coupling effects, this will be the major direction for the future development of the model.

REFERENCES

1. A. L. Loeb, Thermal conductivity: VIII. A theory of thermal conductivity of porous materials, *J. Am. Ceram. Soc.* **37**, 96–99 (1954).
2. J. C. Maxwell, *A Treatise on Electricity and Magnetism*, 3rd Edn, Vol. I, Chap. 9, Article 314. Dover, New York (1954).
3. J. C. Y. Koh and A. Fortini, Thermal conductivity and electrical resistivity of porous material, NASA Report No. NAS3-12012, CR-120854 (1971).
4. H. W. Russell, Principles of heat flow in porous materials, *J. Am. Ceram. Soc.* **18**, 1 5 (1935).
5. A. Eucken, Thermal conductivity of ceramic refractory materials; calculation from thermal conductivity of constituents, *Forsch. Geb. Ing Wes.* B3, Forschungsheft No.

353, 16 (1972). *Ceramic Abstr.* **11**, 576 (1932); **12**, 231 (1933).
6. J. Francl and W. D. Kingery, Thermal conductivity: IX. Experimental investigation of effect of porosity on thermal conductivity, *J. Am. Ceram. Soc.* **37**, 99–107 (1954).
7. M. Murabayashi, S. Namba, Y. Takahashi and T. Mukaibo, Effect of porosity on the thermal conductivity of ThO_2, *J. Nucl. Sci. Technol.* **6**, 128–131 (1969).
8. J. S. Agapiou and M. F. DeVries, An experimental determination of the thermal conductivity of a 304L stainless steel powder metallurgy material, *ASME J. Heat Transfer* **111**, 281–286 (1989).
9. S. A. El-Fekey, Y. M. El-Mamoon and M. N. A. El-Hakim, Mathematical analysis of the dependence of thermal conductivity on porosity, *Powder Metall. Int.* **37**, 80–81 (1978).
10. A. D. Stuckes and R. P. Chasmar, Measurement of the thermal conductivity of semiconductors, Report of the Meeting of Semiconductors, Phys. Soc., London, pp. 119–125 (1956).
11. D. R. Williams and H. A. Blum, Thermal conductivities of several methods: an evaluation of a method employed by the NBS, *Proc. 17th Conf. on Thermal Conductivity*, NBS 302, pp. 349–354 (1967).
12. V. V. Mirkovich, Comparative method and choice of standards for thermal conductivity determinations, *J. Am. Ceram. Soc.* **48**, 387–391 (1965).
13. D. R. Flynn, Thermal conductivity of ceramics in mechanical and thermal properties of ceramics, *NBS Spec. Publ.* **303**, 104 (1969).
14. M. J. Laubitz, *Thermal Conductivity* (Edited by R. P. Tye), Vol. 1. Academic Press, London (1969).
15. R. P. Tye, *Thermal Conductivity* (Edited by R. P. Tye), Vol. 2. Academic Press, London (1969).
16. D. Y. Tzou and E. P. Chen, Overall degradation of conductive solids with mesocracks, *Int. J. Heat Mass Transfer* **33**, 2173–2182 (1990).
17. B. Budiansky, On the elastic moduli of some heterogeneous materials, *J. Mech. Phys. Solids* **13**, 223–227 (1965).
18. B. Budiansky, Thermal and thermoelastic properties of isotropic composites, *J. Compos. Mater.* **4**, 286–295 (1970).
19. B. Budiansky and R. J. O'Connell, Elastic moduli of a cracked solid, *Int. J. Solids Structures* **12**, 81–97 (1976).
20. H. Horii and S. Nemat-Nasser, Overall moduli of solids with microcracks: load-induced anisotropy, *J. Mech. Phys. Solids* **31**, 155–171 (1983).
21. A. L. Florence and J. N. Goodier, Thermal stress at spherical cavities and circular holes in uniform heat flow, *ASME J. Appl. Mech.* **26**, 293–294 (1959).

EFFET SUR LA CONDUCTIVITE THERMIQUE APPARENTE DU TRANSFERT DE CHALEUR INTERNE DANS DES CAVITES

Résumé—A l'aide d'un modèle analytique, on étudie la dégradation de la conductivité thermique apparente en tenant compte du mécanisme interne du transfert thermique entre le milieu solide et le fluide dans les cavités. Celles-ci sont supposées être distribuées au hasard dans le solide avec une densité mesurée par la fraction volumique. Le modèle est capable de caractériser l'effet du transfert de chaleur interne par conduction et convection à travers les surfaces des cavités. Pour le mode convectif, le nombre de Biot est identifié comme étant le module déterminant la conductivité tandis que dans le mode conductif le facteur principal est le rapport de la conductivité thermique du solide à celle du fluide dans les cavités. L'effet de la conduction interfaciale et de la convection est prononcé lorsque la fraction volumique des pores dans le solide dépasse 15%. Le grand écart aux résultats expérimentaux quand on considère les cavités comme isolées est rattrapé en considérant les bilans de conduction et convection à travers les surfaces des cavités.

DER EINFLUSS DES INNEREN WÄRMEÜBERGANGS IN HOHLRÄUMEN AUF DIE GESAMTWÄRMELEITFÄHIGKEIT EINES PORÖSEN MEDIUMS

Zusammenfassung—Auf der Grundlage eines analytischen Modells wird in der vorliegenden Arbeit die Abnahme der Gesamtwärmeleitfähigkeit aufgrund des inneren Wärmeübergangs zwischen dem festen Medium und dem Fluid in einem Hohlraum untersucht. Es wird angenommen, daß der Hohlraum auf zufällige Weise im Feststoff verteilt ist. Seine Dichte wird durch den Volumenanteil charakterisiert. Das Modell ist in der Lage, den Einfluß des inneren Wärmeübergangs infolge Leitung und Konvektion an der Hohlraumoberfläche zu beschreiben. In Fällen, bei denen die Konvektion eine Rolle spielt, ist die Biot-Zahl die für die Gesamtwärmeleitung charakteristische Kenngröße, während im Fall überwiegender Wärmeleitung das Verhältnis der Wärmeleitfähigkeiten von Feststoff und Fluid im Hohlraum die wesentliche Einflußgröße ist. Der Einfluß von Wärmeleitung und Konvektion über die Grenzfläche erweist sich als bedeutsam, sobald der Volumenanteil der Poren im Feststoff 15% überschreitet. Die große Abweichung gegenüber Versuchswerten wird behoben, wenn statt isolierter Hohlräume eine Wärmebilanz aufgrund von Leitung und Kovektion über die Hohlraumoberfläche betrachtet wird.

ВЛИЯНИЕ ВНУТРЕННЕГО ТЕПЛОПЕРЕНОСА В ПОЛОСТЯХ НА КОЭФФИЦИЕНТ СУММАРНОЙ ТЕПЛОПРОВОДНОСТИ

Аннотация—На основе аналитической модели исследуется снижение коэффициента суммарной теплопроводности за счет внутренних механизмов теплопереноса между твердой средой и жидкостью в полостях. Предполагается, что полости хаотически распределены в твердом теле, а их плотность определяется объемной долей. Модель может характеризовать влияние внутреннего теплопереноса, в частности, такого как конвективный и кондуктивный теплоперенос через поверхности полостей. В случае конвективного режима число Био является величиной, определяющей коэффициент суммарной теплопроводности, в то время как при кондуктивном режиме основным определяющим фактором является отношение коэффициентов теплопроводности твердой среды и жидкости внутри полостей. Найдено, что эффект теплопроводности и конвекции на межфазной границе особенно заметен, когда объемная доля пор в твердой среде превышает 15%. Существенное отклонение от экспериментальных результатов, полученное при исследовании изолированных полостей, устраняется посредством учета теплового баланса конвекции или теплопроводности через поверхность полости.